

An Improved Method of Pre-Filter Based Image Watermarking in DWT Domain

¹Somnath Maiti, ²Arindam Bose, ³Chirag Agarwal, ⁴Subir Kumar Sarkar, ⁵Nurul Islam

^{1,2,3}Future Institute of Engineering and Management, Kolkata, WB, India

⁴Jadavpur University, Kolkata, India

⁵Ramakrishna Mission Residential College, Kolkata, WB, India

Abstract

In recent years the study of watermarking using CDMA technique in transform domain is a widely popular method. We incorporated modification in existing algorithm with improved imperceptibility of embedded image while making it capable to extract the hidden image by using correlation technique. The original cover image is decomposed in two stages, firstly into appropriate mid-frequency sub-band and secondly into three hierarchical levels of DWT. The logo image is scrambled by PN sequence and then it is embedded in the decomposed cover image. The wavelet coefficients are chosen experimentally for better imperceptibility and robustness against intentional attacks. The result shows a remarkable improvement over the existing methods using similar technique.

Keywords

CDMA, Digital Watermarking, DWT, Sub-band Decomposition

I. Introduction

With the increasing importance of digital media, it has become a common practice to copy, transmit and distribute digital information in communication channel. However it also brings new challenges as it is now very easy to duplicate or even manipulate multimedia content. There is a strong need for protection of intellectual property of owners, creators and distributors. Digital image watermarking has been proposed as valid solution for this problem and it is one such technology that has been developed to protect digital images from illegal manipulations. It is now well established means to embed copyright protection into the digital contents by making small modifications to them. This prevents unauthorized removal of embedded watermarks so that counterfeit copy and distribution can be prevented.

Researches for DWT domain watermarking started since 1997 (Swanson et al. 1997). It is still flourishing in this field (Barni et al. 2001, Wang et al. 2002, Nikolaodis and Pitas et al. 2003, and Serdeen et al. 2003). In recent years researchers have proposed several methods for CDMA based watermarking [2, 4, 9], and [8]. Our proposed method is an attempt to enhance the robustness of existing algorithms as proposed in [2] and [4]. This paper presents a new and efficient method for embedding the watermark in the wavelet domain. We decompose the cover image into various sub-bands using classical Band-Pass Filter. A particular sub-band is selected and 3-Level Selective Discrete Wavelet Transform (DWT) is performed. Then the horizontal and vertical details of wavelet coefficients are selected for embedding the watermark. The watermark message is spread using a Pseudo-Noise (PN) sequence. The watermark image is detected using correlation detector. The algorithm proposed in paper is highly secure and works very well with various attacks like 3×3 Low Pass Filtering, JPEG compression, resizing, and different noises like Gaussian, Poisson Speckle and Salt & Pepper noise.

This paper is organized as follows: In section II we discussed about Related Works in relevant area. In section III we described

about our proposed watermarking model. The algorithm of watermark embedding and extracting are discussed in section IV and V respectively. Section VI demonstrates the experimental results and analyses the performance. Section VII summarizes and concludes this paper.

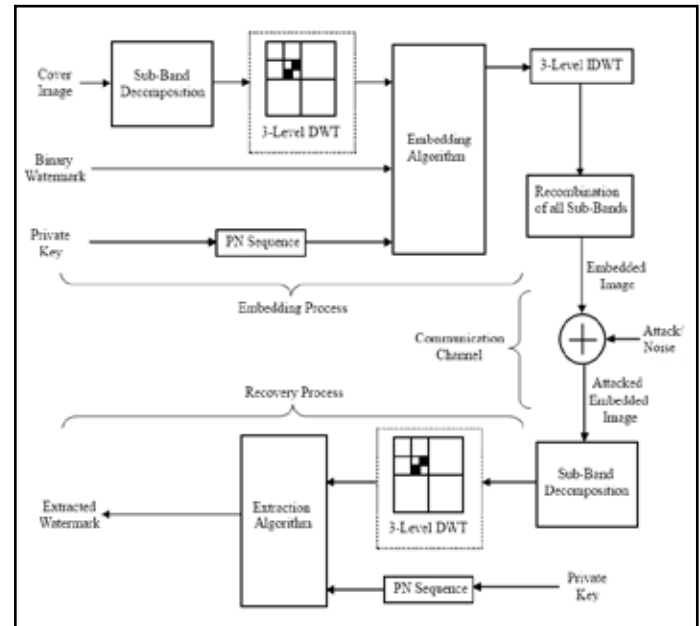


Fig. 1: Block Diagram of Watermark Embedding and Recovery Process

II. Related Works

Several digital watermarking algorithms have been proposed with different contributions. Roughly, these contributions can be categorized according to their processing domain, payload and hiding position. One of the most well-known processing domains is the spread spectrum method proposed by Cox, Kilian, Leighton, and Shamoon (Cox et al. 1996, Cox et al. 1997). The term spread spectrum is used to name this method because according to the authors the watermark is spread throughout the image. Another important feature of this watermark is that it appears like the White Gaussian Random Variable. In the following paragraphs we will go through the brief review of the related works.

N. H. Divecha et al. used 1-level DWT, DCT and SVD transform successively on a 256×256 cover image in their algorithm [3]. They received the correlation between the original watermark and recovered watermark from an un-attacked watermarked image at most 0.9992. They embedded a PN sequence into an image and used it as a secondary watermark image and it was embedded into the final cover image. Although they got relatively high PSNR (dB) but the watermarked image was not robust enough to defend several attacks.

Several papers use 3-level normal DWT as their basic watermarking method. N. Deng et al. used 3-level DWT based watermarking algorithm along with three spread spectrum sequences viz. Wavelet Sequence ($G^W_{24 \times 128}$), Hada Ma Matrix ($G^h_{24 \times 128}$) and Improved

Gold Code Matrix ($G^g_{24 \times 128}$) [4]. M. S. Hsieh et al. also tested their method using 3-level DWT and Embedded Zerotree Wavelet (EZW) and received PSNR as about 44.2 dB [5].

X. Kang et al. proposed a DWT-DFT based method which is robust to Affine Transform and JPEG Compression but not to median filtering attack [7]. Y. Fang et al. suggested a CDMA based watermarking method which is robust to cropping attack, JPEG compression and Gaussian Noise attacks but the performance against geometrical attacks like rotation and scaling is not good enough [8]. They used Bi-orthogonal Wavelets in the HL_1 for second level decomposition. But the watermarked image suffers from lower imperceptible errors and higher Bit Error Rate (BER). Y. Wang et al. used 4-level DWT and decomposed the HH layer in last three decomposition scheme [9].

In this paper we have proposed a simple solution to the short comings as discussed above. The proposed technique is justified by the results obtained from extensive experiments. The algorithm is tuned experimentally by making a trade-off between imperceptibility, robustness and payload.

III. Proposed Watermarking Model

The proposed method employs a frequency band decomposition of the cover image as the first stage of embedding. This pre-filtering helps in achieving a higher imperceptibility level because we are concentrating our focus on the Mid-frequency Band, rather than the whole frequency band. After selecting a particular frequency band of the cover image we perform Multi-level Selective Discrete Wavelet Transform (DWT). We perform a 3-level selective DWT as this method shows the best performance among all its counterparts. 1-level and 2-level DWTs are not enough imperceptible and attack resilient in nature. Hence, multi-level DWT are favored. Both the embedding process and recovery process are described below along with the proposed algorithm. Watermark embedding and detection process is shown in fig. 1.

A. Sub-Band Decomposition

In the very beginning, instead of using the whole span, the cover image is decomposed into some frequency bands to select a specific band for embedding.

Each image f contains details of different frequencies:

$$f \Rightarrow (\Delta_0 f, \Delta_1 f, \Delta_2 f, \dots, \Delta_s f)$$

where,

Δ_0 = Low Pass Filter,

$\Delta_1, \Delta_2, \dots, \Delta_{s-1}$ = Band-Pass Filter,

Δ_s = High Pass Filter, as,

$s + 1$ = Total number of sub-bands.

The original image f can be recombined from those sub-bands using (1).

$$f = \sum_{i=0}^s \Delta_i(\Delta_i f) \tag{1}$$

where, total energy in the image signal f is preserved through (2).

$$\|f\|_2^2 = \sum_{i=0}^s \|\Delta_i f\|_2^2 \tag{2}$$

In this paper, we have decomposed the cover images into the following sub-bands namely, Lower Sub-Band (0-0.2), Lower-Middle Sub-Band (0.2-0.5), Upper-Middle Sub-Band (0.5-0.8) and Upper Sub-Band (0.8-1.0) and chosen the Lower-Middle Sub-Band for embedding since it yields better robustness result as discussed in Section VI. Fig. 2 shows the various sub-band components of Cameraman Image.

B. Discrete Wavelet Transform

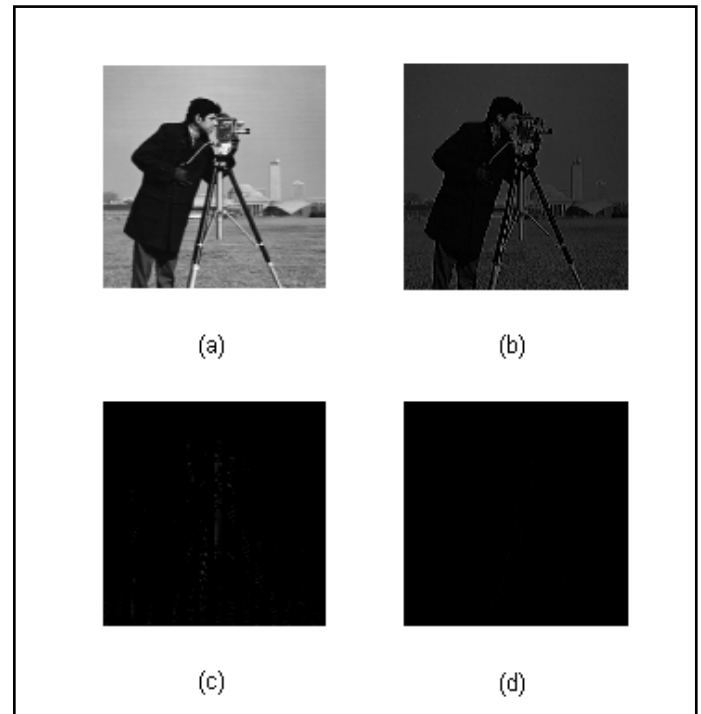


Fig. 2: (a) Lower Band (0-0.2), (b) Lower-Middle Band (0.2-0.5), (c) Upper-Middle Band (0.5-0.8) and (d) Upper Band (0.8-1.0)

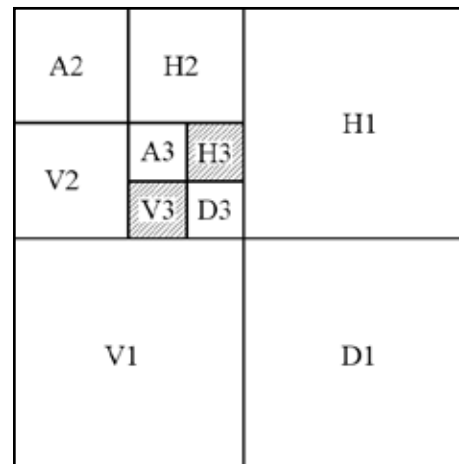


Fig. 3: 3-Level Selective DWT Decomposition Scheme: The Shaded Regions Represent the Embedding Locations

As the image is two-dimensional signal, it needs a 2-dimensional Wavelet Transform in rows and columns, respectively. Image is broken down into four parts quarter size of the sub graph by discrete Wavelet transform, that are high - frequency detail in sub graph and low - pass approximation of sub graph horizontally, vertically and diagonally, each child diagram is received by interval sampling filter. Similar to classical DWT, 2D DWT is a non-redundant transform, the wavelet image representation of f at resolution J :

$$[a_j, \{d_j^1, d_j^2, d_j^3\}]_{0 < j \leq J}$$

having the same size as the original two-dimensional signal, f . We have employed 3-level Selective Haar DWT as it yields best results, which is detailed in experimental result section. Initially we have decomposed our cover images into four DWT coefficients, then we have further decomposed the approximation coefficient $'LL'(a)$ again into four second level DWT coefficients and finally taking the diagonal or $'HH'(d^3)$ details, we have decomposed it

into four third level DWT coefficients. Then we have embedded the watermark information into the ' LH ' (d^1) the horizontal details and ' HL ' (d^2) the vertical details coefficients of the currently decomposed image. Figure 3 describes the decomposition scheme used in our algorithm and Figure 4 shows the different coefficient images of our sample cover image 'Camerman'.

C. Generating PN Sequence and CDMA Encoding



Fig. 4: Different DWT Coefficients of Cover Image Camerman

In CDMA system, the application of PN sequence is purposed on combining the signals of multi-users and keeping them independent. It has the obvious and natural advantage to apply its principles to digital watermarking. We considered this advantage by embedding initially a 16×16 pixels binary watermark image into different cover images having resolution of 512×512 pixels.

Let the watermark message be represented in binary form as $\vec{b} = (\vec{b}_1, \vec{b}_2, \dots, \vec{b}_M)$, where $\vec{b}_i \in \{0,1\}$ and M denotes the number of bits in the watermark information to be encoded. The PN sequence generated using the unique private key chosen by both embedding and decoding, and is directly correlated with the binary message to be embedded into the DWT coefficients of the cover images. As we earlier stated that we are using the horizontal and vertical detail coefficients of 3-level Selective DWT of the cover images having resolution of $M_c \times N_c$ pixels, we need to generate a PN sequence having size $M_c/2^3 \times N_c/2^3$. So in this scenario, our algorithm also limits the size of the watermark image to be at the maximum of $M_c/2^3 \times N_c/2^3$.

For the encoding process we have employed an embedding strength (k) which determines the degree of correlation between the wavelet coefficient and the generated PN sequence. In our algorithm, when the encoder detects a '0', it correlates the coefficient with the PN sequence multiplying it with k . If it detects a '1', nothing is correlated and thereby it reduces the encoder complexity.

Our model follows exactly the reverse methodology to recover the embedded watermark in the cover images. While extracting the watermark, we have initially taken a full white or unit matrix having size exactly same as the original watermark. Thus we only need to decide the positions of black pixels for successfully recovery of the watermark.

IV. Watermark Embedding Algorithm

Step 1: The cover image is decomposed into various frequency bands and then chooses a specific band for further operations.

Step 2: The selected frequency sub-band is decomposed into three level Selective DWT coefficients according to the proposed scheme. Out of the four sub-bands, only the high resolution bands (H_3 sub-band or HL_3 coefficient and V_3 sub-band or LH_3 coefficient) are selected for embedding.

Step 3: A highly uncorrelated, zero-mean, two-dimensional Pseudorandom Sequence (PN) of the size of sub-band matrix is generated using a particular key for each zero bit of the watermark image.

Step 4: Embed the same PN sequence in the selected DWT coefficients H_3 and V_3 with the embedding strength (k) using the following formula:

If $watermark(i) = 0$,

$$\widehat{H}_3 = H_3 + k * PN \text{ sequence}$$

$$\widehat{V}_3 = V_3 + k * PN \text{ sequence}$$

If $watermark(i) = 1$,

$$\widehat{H}_3 = H_3$$

$$\widehat{V}_3 = V_3$$

where,

$$1 \leq i \leq \text{length}(\text{watermark})$$

(3)

Step 5: Perform 3-level IDWT on the transformed image in the reverse way to get back the desired form.

Step 6: Recombine all the frequency sub-bands, along with multiplying the chosen frequency band with an intensity recovering factor (g).

Fig. 4 shows the different coefficient images of our sample cover image 'Camerman'.

V. Watermark Extraction Algorithm

Step 1: The received watermarked image is again decomposed into some frequency sub-bands and the same sub-band is chosen for further operations. The received watermarked image can be preceded by attack on the image like different kinds of noises, JPEG compression, low pass filter etc. in order to evaluate the performance of the procedure better.

Step 2: Apply three-level Selective DWT to the selected sub-band and select the same sub-band into which the watermark was embedded.

Step 3: Regenerate the PN sequence using the same key which was used in the embedding section.

Step 4: Calculate the correlation coefficient between the above selected sub-bands and the regenerated PN sequence.

Step 5: Calculate the mean of all the correlation values obtained above and compare it with each correlation value with the mean correlation value. If the calculated correlation value is greater than the mean, the extracted watermark bit is taken as zero, otherwise one. The recovery process is then iterated through the entire PN sequence.

Step 6: The watermark is constructed using the extracted watermark bits, and then in order to check the likeliness of the original and extracted watermark we compute the Similarity Ratio or Correlation and Bit Error Rate between them.

VI. Experimental Results

A. Justification of Proposed Watermark Algorithm

To verify the effectiveness and versatility of our proposed method we have applied our embedding algorithm to a large number of cover images. We are showing results for only five grey scale images:

1. Cameraman,
2. Lake,
3. Lena,
4. Mandrill and
5. Peppers,

each having size of 512×512 pixels. All the watermarked images which are embedded with the given watermark through our proposed watermarking method are shown in Table 1. It is clear that visually the images are imperceptible. The watermark has been embedded into all the five different cover images using the respective values of embedding strength (k), for whose minimum value, the Bit Error Rate (BER) is maximum i.e. ‘1’.

Table 1: Original Cover Image, Watermarked Image and Extracted Watermark of Cover Images: (a) Cameraman, (b) Lake, (c) Lena, (d) Mandrill and (e) Peppers.

	Original Image	Embedded Watermark	Watermarked Image
(a)			
(b)			
(c)			
(d)			
(e)			

We also compared various forms of three level DWT, viz. Normal 3-level DWT, Normal 3-level DWT with sub-band decomposition, Selective 3-level DWT with sub-band decomposition for the cover image Cameraman. A graphical comparison among the above three forms is shown in fig. 5. It is clearly observed from the fig. that the normal 3-level DWT gives good performance with respect to Correlation but performs very poorly as far as PSNR is concerned, whereas, in Selective 3-level DWT it is seen that for a Correlation factor of 0.965 we get sufficiently high PSNR but it then drastically falls as the former tends to 1. This defect is corrected by using Sub-Band Decomposed Selective DWT, which provides the most stable curve amongst all.

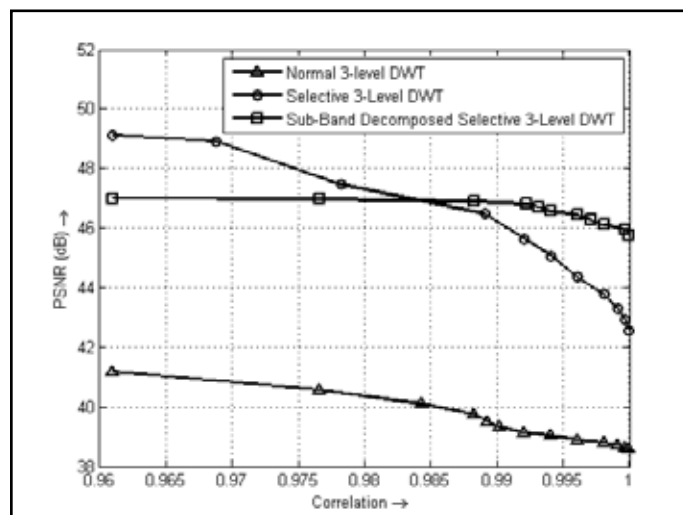


Fig. 5: Graph of Correlation Against PSNR (dB) for Normal 3-Level DWT, Selective 3-Level DWT and Sub-Band Decomposed Selective 3-Level DWT of Cameraman. The Graph Indicates that the Selective 3-Level DWT Yields the Efficient Result

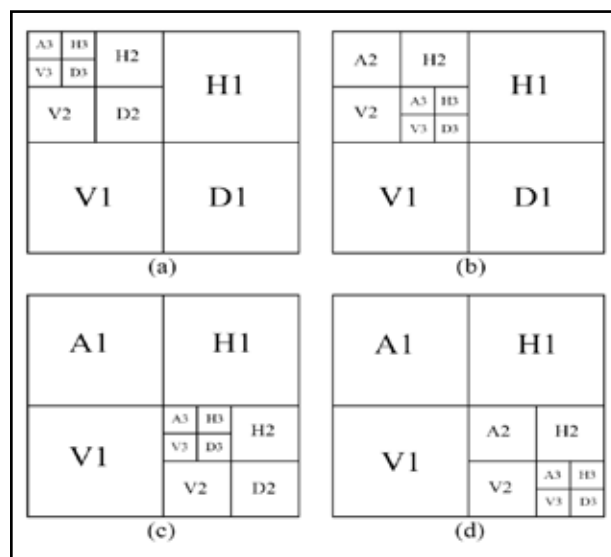


Fig. 6: Different Possible Regions of 3-level DWT: (a) Region 1, (b) Region 2, (c) Region 3, (d) Region 4

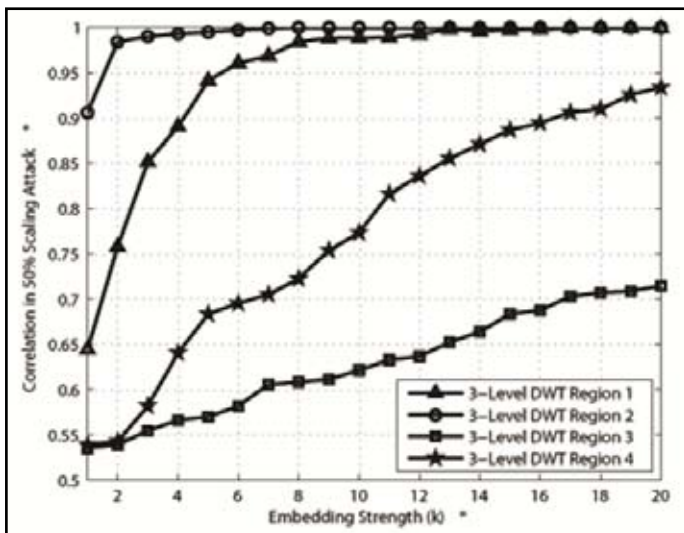


Fig. 7: Graph of Embedding Strength Against Correlation of 50% Scaling Attack for Various Regions of 3-level DWT of Cameraman. The Graph Indicates that Region 2 Yields Best Result

In our proposed method we have justified the reason for choosing the selective 3-level DWT [Cover Image $\rightarrow A_1 \rightarrow D_2$] region of decomposition of the cover image. We didn't choose the Horizontal (H) or Vertical (V) sub-bands for decomposition because they led to different types of artifact errors which easily visible in the watermarked image and also were less robust. The only four possible decomposition regions are,

- Region 1: Cover Image $\rightarrow A_1 \rightarrow A_2$
- Region 2: Cover Image $\rightarrow A_1 \rightarrow D_2$
- Region 3: Cover Image $\rightarrow D_1 \rightarrow A_2$
- Region 4: Cover Image $\rightarrow D_1 \rightarrow D_2$

as depicted in fig. 6. Region 1 is identified as Normal 3-level DWT and we use Region 2 in our Selective DWT algorithm.

Figure 7 shows the graph of Embedding Strength (k) against Correlation of 50% Scaling Attack for various regions of 3-level DWT of Cameraman. Both region 1 and region 2 show similar characteristics considering their performance against such attacks for $k > 12$, but for $k < 10$ region 2 gives better performance. Comparing the PSNR values of region 1 and region 2 from Figure 5 also reveals the superiority of region 2 over region 1. It is clearly observed in Figure 7 that both region 3 and region 4 show very poor performance against attacks. Thus, region 2 gives the best performance in both the cases, hence our choice.

B. Robustness Analysis

Robustness holds a high degree of importance in any watermarking algorithm. In our experiments, the watermark and the PN sequence are embedded into five different gray images. We tested various kinds of attacks on our cover images, such as:

- 3x3 Low Pass Filter,
- Gaussian Noise of variance 0.01,
- Salt & Pepper Noise of variance 0.1,
- Speckle Noise of variance 0.1,
- JPEG Compression for $Q = 50$,
- 50% Scaling attack,
- Histogram Equalization of 32 step-size.

By increasing the level of attacks introduced to an embedded image we see that the respective BER value obtained is very low, then we can conclude that the algorithm is highly robust. It can

sustain strong attacks and still be able to recover the watermark accurately. The corrupted watermarked image and the extracted watermark as observed for the cover image 'Cameraman' are shown in fig. 8.

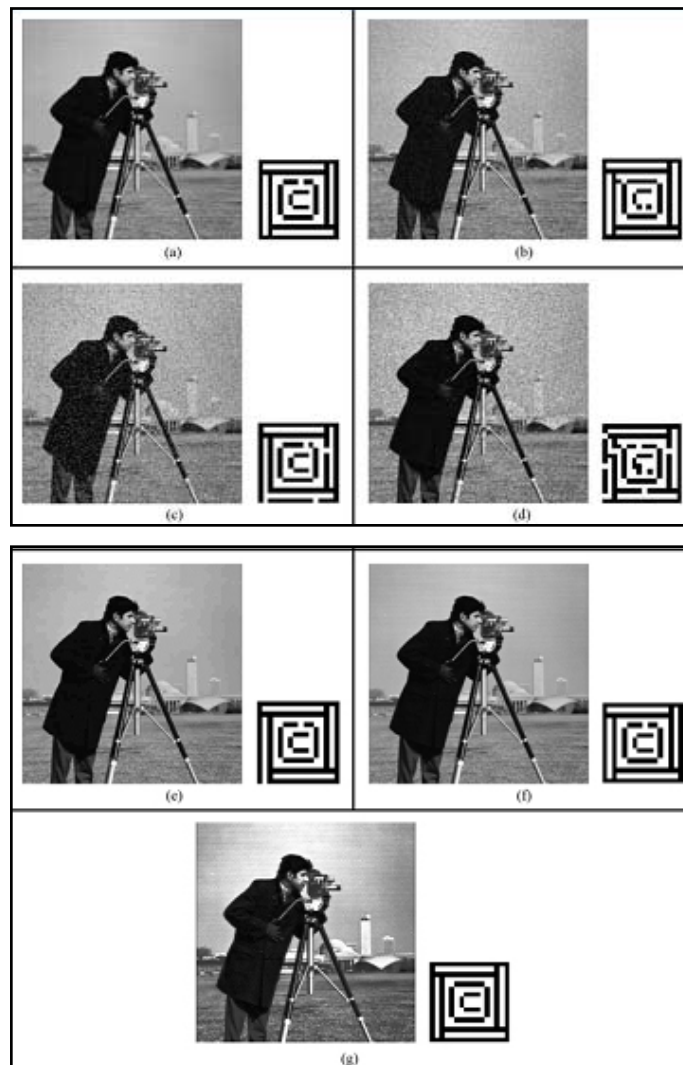


Fig. 8: Attacked Watermarked Images and Their Respective Recovered Watermarks: (a) 3x3 Low Pass Filter, (b) Gaussian Noise of Variance 0.01, (c) Salt & Pepper Noise of Variance 0.1, (d) Speckle Noise of Variance 0.1, (e) JPEG Compression of $Q = 15$, (f) 50% Scaling Attack, (g) Histogram Equalization of 32 Step-Size

It is clear from fig. 8, that the subjective watermark is recovered almost accurately for all the attacks, and hence the proposed method is robust against attacks. This is further verified by analyzing the nature of the Bit Error Rate curve against some of the attacks. In fig. 9 we analyzed the Salt & Pepper Noise Density (d) vs. BER graph in which we observe that even if we increase d to as high as 0.1 we get a BER around 0.02-0.04 for all the five cover images, indicating the highly robust nature of the algorithm.

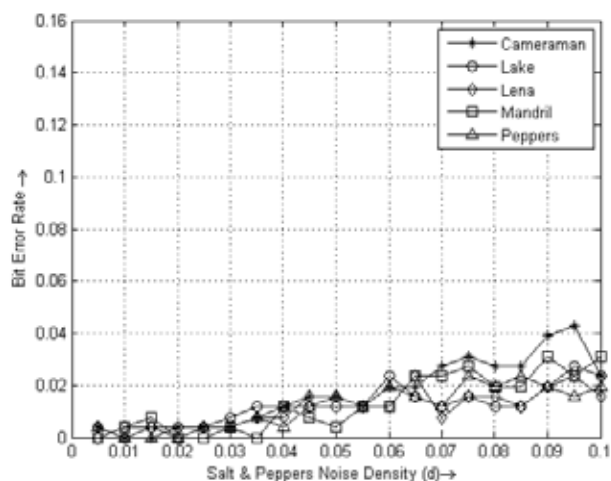


Fig. 9: Curve of Bit Error Rate (BER) Against Varying Density of Salt & Pepper Noise (d) for Different Cover Images. The Curve Indicates that with Rapid Increasing d , BER Increases with a Very Slow Rate

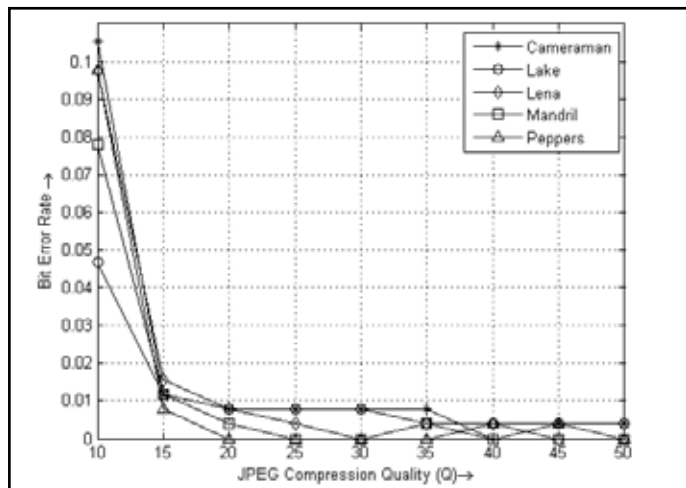


Fig. 10: Curve of Bit Error Rate (BER) against varying Quality Factor of JPEG Compression (Q) for Different Cover Images. The Curve Indicates that from $Q = 10$ to $Q = 15$ BER Falls Drastically and After $Q = 15$, BER Decreases in a Very Slow Rate and Often Tends to Zero

In fig. 10, we analyzed the BER curve for the Quality Factor of JPEG Compression (Q) varying from 10 to 50, indicating a 10-50% compression of the image. Y. Fang et al. took a 1024 bit watermark in their algorithm and achieved a fair amount of robustness for both Lena and Mandrill [8]. We compared our result in which we took a 2048 bit watermark at different Quality factor of JPEG Compression. It is observed that our proposed algorithm shows better robustness against JPEG Compression. Bit Error Rate as observed is very low as compared to theirs. JPEG Compression is treated as one of the important noise parameters and by observing the results it can be inferred that it performs well against the same.

C. Quality Analysis

1. Peak Signal to Noise Ratio (PSNR)

PSNR is considered an important tool in order to comment on the quality of the embedded image. In fig. 11 the graph describes the nature of PSNR values of the five different cover images with increasing values of Embedding Strength (k). The graph follows

the obvious nature, i.e. the higher is the value of k , the higher is the degree of information embedded in the cover image and hence is lower the PSNR value.

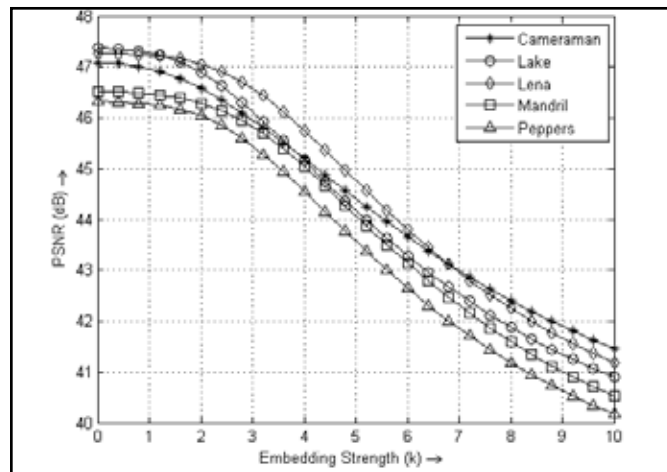


Fig. 11: Curve of Peak Signal to Noise Ratio (PSNR) in dB Against Varying Embedding Strength (k) for Different Cover Images. The Curve Indicates that with Increasing k , PSNR Decreases

2. Bit Error Rate (BER)

BER is another important metric which gives valuable information about the recovered watermark. BER is a measure of the error between the original and the recovered watermark. In fig. 12 the graph describes the nature of BER values of the five different cover images with increasing values of Embedding Gain Factor (k). A very important thing can be concluded on observing the graph; we see that every cover image shows a somewhat different nature towards the values of k . On one hand, images like Peppers and Cameraman gives a BER as low as 0.01-0.02 whereas, for the same value of k , images like Mandrill gives a BER of 0.1 for the same value of k . So if we take an average value then it can be said that for $k = 3$ we are able to recover the watermark from all the images.

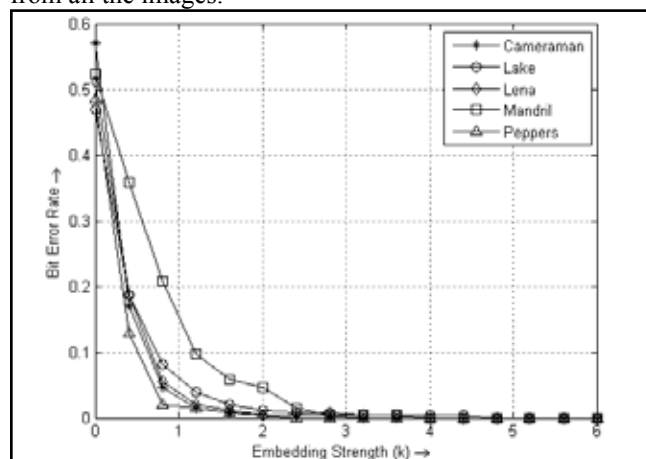


Fig. 12: Curve of Bit Error Rate (BER) Against Varying Gain of Embedment (k) for Different Cover Images. The Curve Indicates that with Increasing k , BER Decreases Rapidly

3. Payloads (Bytes)

An algorithm which supports higher payload is given more preference, but it is also important to analyze the nature of PSNR and BER curves against increment of the payload. However, we see that even if we increase the payload, we still obtain better results. We have taken other watermark images of varying pixels size and payloads (in bytes).

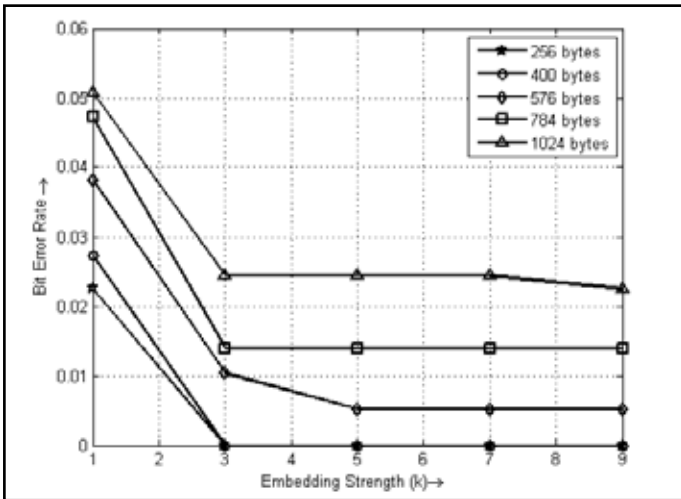


Fig. 13: Curve of Bit Error Rate (BER) Against Embedding Strength (k) for Different Watermark Images Having Different Size and Payloads. The curve Indicates that from k = 1 to k = 3 BER Falls Drastically and After k = 3, BER Decreases Almost in a Straight Line. The Curve Also Indicates that for Same , BER Increases With Increasing Payloads

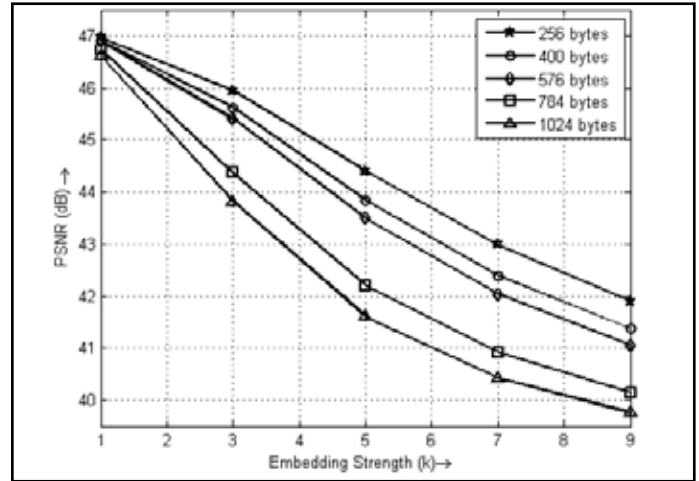


Fig. 14: Curve of Peak Signal to Noise Ratio (PSNR) in dB Against Embedding Strength (k) for Different Watermark Images Having Different Size and Payloads. The Curve Indicates that with Increasing k, PSNR Decreases Almost in a Constant Slope. The Curve Also Indicates that for Same k, PSNR Decreases with Increasing Payloads

We observe that if we take a 32x32 watermark (original watermark was a 16x16 image) we still are able to recover the watermark with a BER of as low as around 0.03, i.e. we are able to recover 99.97% of the hidden watermark. Fig. 13 and fig. 14 show the nature of BER and PSNR with increasing value of k for different payloads so as to comment on the proposed algorithm.

If we take an average of both the graphs the we can conclude that for all the payloads we get very low values of BER which is always less than 0.05, and the PSNR value is always higher than 40dB.

4. Other Test Matrices

Different performance metrics are calculated to estimate the quality and authenticity of an embedded image with respect to the cover image. Test metrics including,

- Normalized Cross Correlation (NC),
- Correlation Quality (CQ),
- Image Fidelity (IF),
- Pearson Correlation Coefficient (PCC),
- Average Absolute Difference (AD),
- Normalized Mean Square Error (NMSE),
- Structural Content (SC)

are calculated for each of the cover image for different values of Embedding Strength (k), and are given in Table 2.

Table 2: Various Test Metrics for Watermarked Image

Cover Image	k ↑	NC↓	CQ↓	IF↓	PCC↑	AD↑	NMSE↑	LMSE↑	SC↑
Cameraman	2.9	0.013347	2.0128	0.99985	0+1.8923i	7.0092	0.00014798	0.50930	74.2040
	5	0.013304	2.0062	0.99969	0+1.8923i	7.7441	0.00031066	1.41480	74.6224
	8	0.013236	1.9959	0.99922	0+1.8924i	9.3990	0.00078437	3.49040	75.1986
Lake	4.7	0.012893	2.0493	0.99978	0+1.8812i	7.7628	0.00021552	0.27994	77.5809
	6	0.012892	2.0491	0.99963	0+1.8812i	8.3962	0.00036940	0.44366	77.6002
	8	0.012889	2.0486	0.99929	0+1.8812i	9.5866	0.00070561	0.77200	77.6519
Lena	4	0.014425	2.0557	0.99986	0+2.5706i	7.2694	0.00014411	0.47529	69.3254
	5	0.014425	2.0557	0.99977	0+2.5706i	7.6695	0.00022712	0.72805	69.3259
	5.6	0.014425	2.0557	0.99970	0+2.5706i	7.9593	0.00029825	0.90692	69.3264
Mandrill	4	0.014085	1.9844	0.99986	0+3.1930i	7.4853	0.00014206	0.23627	70.9939
	4.5	0.014085	1.9844	0.99982	0+3.1930i	7.6651	0.00017642	0.29463	70.9954
	5.3	0.014084	1.9843	0.99975	0+3.1930i	8.0063	0.00025223	0.40219	70.9983
Peppers	2.4	0.015161	2.1465	0.99990	0+2.1571i	6.5593	0.00009746	0.11532	65.7364
	4	0.015152	2.1451	0.99982	0+2.1571i	7.0234	0.00017677	0.28255	65.8226
	6	0.015134	2.1426	0.99957	0+2.1571i	7.9866	0.00042517	0.60873	65.9634

↑ indicates the corresponding value is increasing when k is increasing, and
↓ indicates the corresponding value is decreasing when k is increasing.

VII. Conclusion

In this paper, we proposed a modification of blind DWT based image watermarking algorithm using CDMA technique. We introduced Selective Sub-Band decomposition along with 3-level DWT in order to enhance the robustness and imperceptibility of the embedded image. Various experimental graphs and table validate our claim in favor of our proposed algorithm. In particular, the results show that the watermarked image is robust to a number of attacks like Low Pass Filtering, JPEG Compression, Scaling, Gaussian Noise, Salt & Pepper Noise, Speckle Noise, Histogram Equalization, Gamma Correction and Intensity Adjustment. DWT suffers from shift sensitivity, hence its performance against Rotation and Cropping is comparatively not satisfactory. In future works, we will investigate on the improvement of Geometrical attacks like Rotation and Cropping and develop a new algorithm for color images.

References

- [1] Y. Fang, J. Huang, Y. Q. Shi, "Image Watermarking Algorithm Applying CDMA", in Proc. Int. Symp. Circuits and Systems, May 25-28, 2003, Vol. 2, pp. II-948-II-951.
- [2] M. K. Samee, J. Götze, "CDMA Based Blind and Reversible Watermarking Scheme for Images in Wavelet Domain", in Proc. 19th Int. Conf. Systems, Signals and Image Processing, April 11-13, 2012, Vienna, Austria, pp. 154-159.
- [3] N. H. Divecha, N. N. Jani, "Image Watermarking Algorithm using DCT, DWT and SVD", presented at the Nat. Conf. on Innovation Paradigms in Engineering & Technology, Nagpur, India, International Journal of Computer Applications, No. 10, March, 2012, pp. 13-16.
- [4] N. Deng, C. Jiang, "CDMA watermarking algorithm based on wavelet basis", in Proc. 9th Int. Conf. Fuzzy Systems and Knowledge Discovery, May 29-31, 2012, pp. 2148-2152.
- [5] M. S. Hsieh, D.C. Tseng and Y. H. Huang, "Hiding Digital Watermarks Using Multiresolution Wavelet Transform", IEEE Trans. Ind. Electron., Vol. 48, No. 5, October 2001, pp. 875-882.
- [6] R. Safabakhsh, S. Zabolli, A. Tabibiazar, "Digital Watermarking on Still Images Using Wavelet Transform", in Proc. Int. Conf. Information Technology: Coding and Computing, April 5-7, 2004, Vol. 1, pp. 671-675.
- [7] X. Kang, J. Huang, Y. Q. Sh, Y. Lin, "A DWT-DFT Composite Watermarking Scheme Robust to Both Affine Transform and JPEG Compression", IEEE Trans. Circuits Syst. Video Technol., Vol. 13, No. 8, August 2003, pp. 776-786.
- [8] Y. Fang, J. Huang, S. Wu, "CDMA-Based Watermarking Resisting to Cropping", in Proc. Int. Symp. Circuits and Systems, May 23-26, 2004, vol. 2, pp. II-25-II-28.
- [9] Y. Wang, J. F. Doherty, R. E. V. Dyck, "A Wavelet-Based Watermarking Algorithm for Ownership Verification of Digital Images," IEEE Trans. Image Process., Vol. 11, No. 2, February 2002, pp. 77-88.
- [10] B. L. Gunjal, R. R. Manthalkar, "Discrete Wavelet Transform based Strongly Robust Watermarking Scheme for Information Hiding in Digital Images", in Proc. 3rd Int. Conf. on Emerging Trends in Engineering and Technology, November 2010, pp. 124-129.
- [11] Y. Fang, N. Bi, D. Huang, J. Huang, "The M-Band Wavelets in Image Watermarking", in Proc. Int. Conf. Image Process., Vol. 1, September 2005, pp. I-245-8.
- [12] S. P. Maity, M. K. Kundu, "A Blind CDMA Image Watermarking Scheme in Wavelet Domain", in Proc. Int. Conf. Image Process. Vol. 4, October 2004, pp. 2633-2636.
- [13] I. J. Cox, J. Killian, F. T. Leighton, T. Shamoan, "Secure Spread Spectrum Watermarking for Multimedia", IEEE Trans. Image Process., Vol. 6, No. 12, December 1997, pp. 1673-1687.